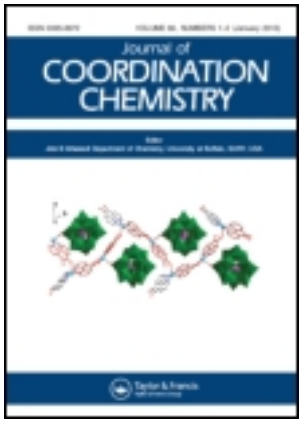

Journal of Coordination Chemistry
Publication details, including instructions for authors and subscription information:
http://www.tandfonline.com/loi/gcoo20

Lanthanide complex of 1-phenyl-3-methyl-5-hydroxypyrazole-4-carbaldehyde-(isonicotinoyl) hydrazone: crystal structure and DNA-binding properties

Mingfang Wang [a] , Zhengyin Yang [a] , Yong Li [a] & Hongge Li [a]
[a] Key Laboratory of Nonferrous Metals Chemistry and Resources Utilization of Gansu Province, College of Chemistry and Chemical Engineering, Lanzhou University , Lanzhou 730000 , P.R. China
Published online: 07 Sep 2011.

To cite this article: Mingfang Wang , Zhengyin Yang , Yong Li & Hongge Li (2011) Lanthanide complex of 1-phenyl-3-methyl-5-hydroxypyrazole-4-carbaldehyde-(isonicotinoyl) hydrazone: crystal structure and DNA-binding properties, Journal of Coordination Chemistry, 64:17, 2974-2983, DOI: 10.1080/00958972.2011.610102

To link to this article: http://dx.doi.org/10.1080/00958972.2011.610102

Journal of Coordination Chemistry
Vol. 64, No. 17, 10 September 2011, 2974–2983

Lanthanide complex of 1-phenyl-3-methyl-5-hydroxypyrazole-4-carbaldehyde-(isonicotinoyl) hydrazone: crystal structure and DNA-binding properties

MINGFANG WANG, ZHENGYIN YANG*, YONG LI and HONGGE LI

Key Laboratory of Nonferrous Metals Chemistry and Resources Utilization of Gansu Province, College of Chemistry and Chemical Engineering, Lanzhou University, Lanzhou 730000, P.R. China

(*Received 16 March 2011; in final form 6 July 2011*)

A Schiff-base ligand derived from 1-phenyl-3-methyl-4-formyl-2-pyrazolin-5-one (PMFP) and isoniazid was prepared and its La(III) complex was characterized by X-ray single crystal diffraction. The La(III) is nine-coordinate in a space group $P2_1/n$. DNA-binding was investigated by UV-Vis, fluorescence titration, ethidium bromide displacement experiments, and viscosity measurements, which indicated that the ligand and La(III) complex strongly binds to calf thymus DNA presumably *via* groove binding and intercalation. The intrinsic binding constants of the ligand and La(III) complex were 0.86×10^5 and $2.46 \times 10^5 \text{ mol L}^{-1}$, respectively. Antioxidant data from hydroxyl radical scavenging experiments *in vitro* suggest that the La(III) complex possesses higher scavenging ratio than the free ligand, metallic salt, and some standard antioxidants like mannitol.

Keywords: La(III) complex; PMFP-isonicotinoyl hydrazone; DNA-binding properties; Antioxidant activities

1. Introduction

Interaction of metal complexes with nucleic acid and their constituents are of interest in bioinorganic chemistry. Cisplatin and its analogs have played a key role as potent antitumor drugs [1]. Cisplatin and many other chemicals exert their antitumor effects through binding to DNA, thereby changing the replication of DNA and inhibiting the growth of tumor cells [2]. In order to synthesize new and more efficient antitumor drugs, it is necessary to understand different binding modes of metal complexes to DNA. Metal complexes interact with DNA in either a non-covalent or a covalent way. The former includes three binding modes: groove binding [3–5], intercalation [6, 7], and external static electronic effects. While most DNA-interacting agents selectively bind to DNA by either groove binding or intercalation, some compounds can exhibit both binding modes. Groove binding is one of the most important DNA-binding modes as it invariably leads to cellular degradation. Intercalating ability increases with the

*Corresponding author. Email: yangzy@lzu.edu.cn

Journal of Coordination Chemistry
ISSN 0095-8972 print/ISSN 1029-0389 online © 2011 Taylor & Francis
DOI: 10.1080/00958972.2011.610102

planarity of ligands; also, coordination geometry including the ligand donor type and the metal ion with flexible valence determine the binding extent of metal complexes to DNA [8].

Some lanthanide complexes with Schiff bases play a major part in bioinorganic chemistry because of their biological and pharmaceutical activities, such as antitumor, antioxidant activities, cytotoxic activity, and DNA-binding affinity [9–11]. Additionally, 4-acyl pyrazolone derivatives are widely utilized in many fields, especially in clinical and analytical applications [12, 13]. In our previous work, we investigated the synthesis and crystal structures of several lanthanide complexes of pyrazolone derivatives [14–16]. For example, 1-phenyl-3-methyl-5-hydroxy-4-pyrazolyl phenyl ketone (PMBP) isonicotinoyl hydrazone and its rare earth complexes possessed antitumor activity and the La(III) complex had cytotoxic activities, with inhibitory rate for leukemia cells (L_{1210}) of 87.1%. Reactive oxygen species (ROS) are generated by normal cellular metabolism and exogenous agents. Under pathological conditions, ROS are over-produced and result in oxidative stress. ROS can real-time generate when the endogenous antioxidant defenses are inadequate [17]. Among all the ROS, hydroxyl radical ($HO^{\bullet}$) is a highly reactive product, implicated with pathogenic processes including carcinogenesis through direct effects on DNA directly and by acting as a tumor promoter [18].

This article is aimed at DNA-binding activity of an analogous ligand and its lanthanide complex for potential application as pharmaceuticals. With increasing interest on understanding DNA-binding modes, 1-phenyl-3-methyl-5-hydroxypyrazole-4-carbaldehyde-isonicotinoyl hydrazone (PMFP-isonicotinoyl hydrazone) and its La(III) complex are prepared and their DNA-binding modes are investigated. Also, the antioxidative activities are determined. The 50% scavenging ratio on hydroxyl radical obtained for the ligand, La(III) complex, $La(NO_3)_3$, and mannitol demonstrate that the La(III) complex exhibits effective antioxidant activity in comparison with the ligand and some classic antioxidants like mannitol.

2. Experimental

2.1. *Materials and instrumentation*

All materials and solvents were of analytical grade and used without purification. PMP and $La(NO_3)_3 \cdot 6H_2O$ were produced in China. Calf thymus DNA (CT-DNA) and ethidium bromide (EB) were purchased from Sigma Chemical Co. All experiments involved with the interaction of the ligand and complex with CT-DNA were carried out in doubly distilled water buffer containing 5 mmol L^{-1} Tris and 50 mmol L^{-1} NaCl and adjusted to pH 7.2 with hydrochloric acid. Solution of CT-DNA in Tris-HCl buffer gave ratios of UV absorbance of 1.8–1.9 : 1 at 260 and 280 nm, indicating that CT-DNA was sufficiently free of protein [19]. The CT-DNA concentration per nucleotide was determined by employing an extinction coefficient of 6600 mol L^{-1} cm^{-1} at 260 nm [20]. The ligand and its La(III) complex were dissolved in a solvent mixture of 1% DMF and 99% Tris–HCl buffer (pH 7.2) at 1.0×10^{-5} mol L^{-1}.

The melting point of the ligand was determined on a Beijing XT4-100X microscopic melting point apparatus (the thermometer was not corrected). Infrared (IR) spectra

were obtained in KBr discs on a Thermo Mattson FTIR spectrophotometer from 4000 to 400 cm^{-1}. ^1H NMR spectra were recorded on a Varian VR 400 MHz spectrometer in DMSO-d^6 with TMS as an internal standard. Conductivity measurement was performed in DMF solution with a DDS-11C conductometer at 25°C. UV-Vis spectra were obtained on a Perkin-Elmer Lambda 35 UV-Vis spectrophotometer. Fluorescence measurements were recorded on a Hitachi RF-4500 spectrofluorophotometer at room temperature. The antioxidant activity was performed in DMF solution with a 721-E spectrophotometer.

2.2. *X-ray crystallography*

A green crystal of the La(III) complex was obtained by slow vapor diffusion of CH_3OH/ether at room temperature. X-ray diffraction data for the crystal were performed with graphite monochromated Mo-Kα radiation (0.71073 Å) on a Bruker Smart-1000 CCD diffractometer and collected by the $\omega/2\theta$ scan technique at 298(2) K. The crystal structure was solved by direct methods. The positions of non-hydrogen atoms were determined from successive Fourier syntheses. Hydrogens were placed in their geometrically calculated positions. The positions and anisotropic thermal parameters of all non-hydrogen atoms were refined on F^2 by full-matrix least-squares techniques with the SHELX-97 program package. Absorption corrections were employed using semi-empirical methods from equivalents.

2.3. *Preparation of H_2L and its La(III) complex*

2.3.1. Preparation of H_2L. Synthetic pathway of H_2L is shown in figure 1. 1-Phenyl-3-methyl-4-formyl-2-pyrazolin-5-one (PMFP) was prepared according to the literature [21, 22]. An ethanol solution containing isoniazid (1.51 g, 11 mmol) was added dropwise to a stirred solution of the PMFP (2.02 g, 10 mmol) in ethanol (40 mL) at 60°C. After the addition, a large amount of yellow precipitate appeared immediately. The reaction

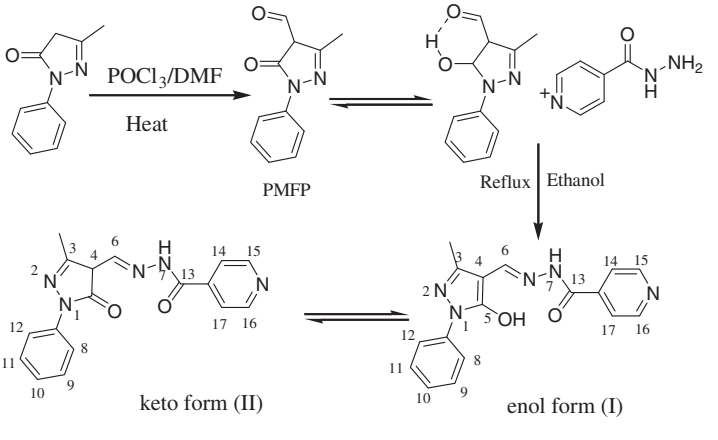

Figure 1. Scheme of the synthesis of the ligand.

mixture was stirred for a further 3 h at this temperature. After that the yellow solution was concentrated and cooled, a yellow solid separated, was filtered, washed, recrystallized from ethanol, and was dried in a vacuum. Yield: 85.15%, m.p. 257–259°C. IR ν_{max} (cm^{-1}): $\nu(C_{(13)}=O)$:1651, $\nu(C=N)$: 1583, $\nu(C_{(5)}=O)=1537$, $\nu(N–H)$: 3132 cm^{-1}. ^1H NMR (400 MHz, DMSO-d^6, ppm): 8.856 (d, 1H, H_7), 8.818 (d, 1H, –OH), 7.973 (d, 1H, H_{15}, $J=8.0$ Hz), 7.915 (d, 2H, H_{14}, H_{16}, $J=8.0$ Hz), 7.877 (d, 2H, H_8, H_{12}, $J=6.4$ Hz), 7.815 (d, 1H, H_{17}, $J=6.4$ Hz), 7.412 (m, 2H, H_9, H_{11}), 7.360 (s, 1H, H_6), 2.211 (s, 3H, CH_3-pyrazole). (The label numbers of hydrogens are shown in figure 1; the 1H spectra is represented in figure S1.)

2.3.2. Preparation of the La(III) complex. H_2L (0.35 mmol, 0.112 g) was dissolved in ethanol (40 mL). After 5 min, an ethanol solution containing La(III) nitrate (0.2 mmol, 0.086 g) was added quickly and the solution was refluxed on a water bath for 12 h with stirring. Then 20 mL distilled water was added dropwise to the reaction solution, after it was concentrated to 5 mL, immediately there was a yellow precipitate in the solution. The precipitate was separated by suction filtration, purified by washing several times with water, and dried for 48 h in a vacuum.

2.4. *DNA-binding studies*

2.4.1. Electronic absorption titration. Electronic absorption titration experiments were performed with fixed concentration of drugs (10 μmol L^{-1}), while gradually increasing the concentration of DNA. When measuring the absorption spectra, an equal amount of DNA was added to both the sample solutions and the reference solution to eliminate absorbance of DNA itself. Each sample solution was scanned from 190 to 500 nm.

2.4.2. Fluorescence spectra. For fluorescence measurements, fixed amounts (10 μmol L^{-1}) of the compounds were titrated with increasing amounts of DNA, over a range of DNA concentrations from 2.5 to 15 μmol L^{-1}. Excitation wavelengths of the samples were about 358 nm. The emission wavelengths were 434 and 421 nm for the ligand and La(III) complex, respectively. Excitation and emission slit were both set at 5 nm. Experiments were conducted at room temperature in a buffer containing 5 mmol L^{-1} Tris–HCl (pH 7.2) and 50 mmol L^{-1} NaCl.

Further support for the mode of the ligand and La(III) complex binding to DNA is given through emission quenching experiments. Quenching data were analyzed according to the Stern–Volmer equation which could be used to determine the fluorescence quenching mechanism:

$$F_0/F = 1 + K_q[Q],$$

where F_0 and F are the fluorescence intensity in the absence and presence of drug at $[Q]$ concentration, K_q is the quenching constant, and $[Q]$ is the quencher concentration. Plots of F_0/F *versus* $[Q]$ appear to be linear and K_q depends on temperature [23].

2.4.3. Viscosity measurements. Viscosity experiments were conducted on an Ubbelodhe viscometer, immersed in a thermostated water bath maintained at

25.0 ± 0.1°C. Titrations were performed for the ligand and complex (0.5–4 μmol L^{-1}), and each compound was introduced into a DNA solution (5 μmol L^{-1}) present in the viscometer. Data were presented as $(\eta/\eta_0)^{1/3}$ *versus* the ratio of the concentration of the compound and DNA, where η is the viscosity of DNA in the presence of the compound and η_0 is the viscosity of DNA alone [24, 25].

2.5. *Antioxidant activity*

In antioxidant activity experiments, hydroxyl radical ($HO^{\bullet}$) in aqueous media was generated through the Fenton reaction [26]. Solutions of the test compounds were prepared with DMF. The reaction mixture contained 2.0 mL 0.15 mol L^{-1} phosphate buffer (pH = 7.4), 1.0 mL 114 μmol L^{-1} safranin, 1 mL 945 μmol L^{-1} EDTA–Fe(II), 1 mL 3% H_2O_2, and 30 μL of test compound solution (final concentration: $C_{i(i=1\text{–}6)}$ = 1.0, 2.0, 3.0, 4.0, 5.0, 6.0 μmol L^{-1}). The sample without the test compound was used as control. The reaction mixtures were incubated at 37°C for 60 min in a water bath. Absorbances (A_i, A_0, A_c) at 520 nm were measured. The scavenging ratio is defined as

$$\text{Suppression ratio (\%)} = [(A_i - A_0)/(A_c - A_0)] \times 100\%,$$

where A_i = absorbance in the presence of the test compound; A_0 = absorbance of the blank in the absence of the test compound; A_c = absorbance in the absence of the test compound, EDTA–Fe(II) and H_2O_2.

The antioxidant activity was expressed as the 50% inhibitory concentration (IC_{50}). IC_{50} values were calculated from regression lines where x was the test compound concentration in μmol L^{-1} and y was percent inhibition of the test compounds.

3. Results and discussion

3.1. *Description of the crystal structure*

The complex crystallizes in the monoclinic lattice with space group $P2_1/n$. Each unit cell contains four molecules (the crystallographic data for the La(III) complex are given in table S1 and selected bond lengths and angles are listed in table S2).

An ORTEP representation of the La(III) complex is shown in figure 2. The La(III) is coordinated by two ONO tridentate ligands (pyrazolone oxygen O7, O13, azomethine nitrogen N2, N11 and hydrazonic oxygen O6, O10). The distances for C21–O13 and C6–O7 are 1.244(9) Å and 1.259(8) Å, respectively, which are between the C–O (1.41–1.44 Å) and C = O (1.19–1.23 Å) distances [27], suggesting that the oxygens of pyrazole coordinate in the enol form. The distances for C21–C37 and C6–C23 are 1.409(11) Å and 1.394(10) Å, respectively, which are between the C–C (1.47–1.53 Å) and C = C (1.32–1.38 Å) distances, supporting the above conclusion. So H_2L is in the enol form (I), losing one proton as a tridentate chelating agent HL^{-1}. One water molecule participates in coordination and the remaining two coordination sites are oxygens of NO_3^-. The analytical results indicate that the crystal structure has a 1 : 2 metal to ligand stoichiometry; however, in papers reported in our group, the general formula of the complexes were $Ln(HL)_3$, with tricapped trigonal prism coordination polyhedra.

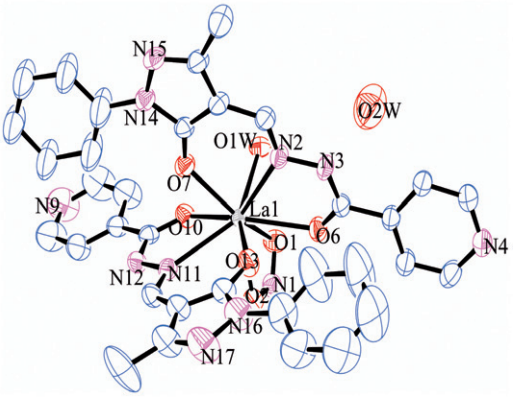

Figure 2. ORTEP view of the La(III) complex showing atom numbering and 30% probability thermal ellipsoids for the non-hydrogen atoms.

The difference might be attributed to bonding of nitrate with lanthanide is stronger than the ligand.

The La(III) complex is air-stable for extended periods and easily soluble in DMF, DMSO, THF, ethanol, and MeOH, slightly soluble in MeCN, and insoluble in water, Et_2O, and acetone. The molar conductivity of the complex is $31.5\,S\,cm^2\,mol^{-1}$, indicating a non-electrolyte [28].

3.2. *IR spectra*

The main IR spectra stretching frequencies are tabulated in table S3. The ligand spectrum shows a medium intensity band at $3132\,cm^{-1}$, assigned to the hydrogen-bonded NH-stretching vibration; the bands at 1651, 1537, and $1583\,cm^{-1}$ are, respectively, allocated as ν(C=O) of the hydrazide, ν(C=O) of the pyrazolone-ring [29], and ν(C=N). These indicate that the ligand exists in the keto form in the solid state. However, in the spectra of the La(III) complex, these bands are at 1619, 1551, and $1457\,cm^{-1}$, respectively, and a new band is observed at $1457\,cm^{-1}$ due to ν(C–O$^-$) [30]. This is consistent with the ligand in the enol form (I) when coordinated to lanthanide. Weak bands at 442 and $627\,cm^{-1}$ are, respectively, allocated as ν(La–N) and ν(La–O). The shifts and new bands further confirmed that nitrogen of imino-group and oxygen of carbonyl form bonds with La(III) [31, 32].

Absorption bands of coordinated nitrate are observed in the preparation of the La(III) complex. The ν_3 free nitrate appears at $1384\,cm^{-1}$ in spectra of the complex. In addition, the separation of the two highest frequency bands $1523\,cm^{-1}$ and $1360\,cm^{-1}$ resulting $|\nu_4–\nu_1|$ is $163\,cm^{-1}$, accordingly the coordinated NO_3^- is bidentate [33]. IR spectra correspond to the crystal structure.

3.3. *DNA-binding studies*

3.3.1. Electronic absorption spectroscopy. Electronic absorption spectroscopy is one of the most universal techniques in DNA-binding studies of metal complexes.

Electronic absorption spectra of the ligand and its La(III) complex in the absence and presence of DNA (at a constant concentration of the compounds) are obtained (figure S2). From the diagram, with increasing DNA concentrations, the absorption bands at 255 nm and 365 nm showed hypochromism, accompanied by a red shift of 4 nm. The reason of the hypochromism may be the $\pi \rightarrow \pi^*$ transitions, and this spectroscopic change indicated strong binding of the ligand and its La(III) complex to DNA. In general, intercalative binding results in hypochromism and red shift due to the strong stacking interaction between an aromatic chromophore and the base pairs of DNA [34]. To compare quantitatively the affinity of the compounds binding to DNA, the intrinsic binding constant (K_b) of the ligand, and La(III) complex were obtained by the electronic absorption spectroscopy. From absorption data, K_b is determined using equation (1) [35] through a plot of [DNA]/($\varepsilon_a - \varepsilon_f$) *versus* [DNA]

$$[\mathrm{DNA}]/(\varepsilon_a - \varepsilon_f) = [\mathrm{DNA}]/(\varepsilon_b - \varepsilon_f) + [K_b(\varepsilon_b - \varepsilon_f)], \quad (1)$$

where [DNA] is the concentration of DNA in base pairs, the apparent extinction coefficients ε_a, ε_f, and ε_b correspond to (A_{obsd}/[compound]), the extinction coefficient for free compound and the extinction coefficient for the compound when fully bound, respectively. In plots of [DNA]/($\varepsilon_a - \varepsilon_f$) *versus* [DNA], K_b is given by the ratio of the slope to the intercept. The intrinsic binding constants K_b of the ligand and La(III) complex are $(0.86 \pm 0.03) \times 10^5$ and $(2.46 \pm 0.02) \times 10^5\,\mathrm{mol\,L^{-1}}$, respectively. These values indicate the La(III) complex has stronger binding affinity than the ligand. The K_b values obtained are lower than those reported for classical intercalators (EB and [Ru(phen)DPPZ] whose binding constants have been found to be on the order of 10^6–$10^7\,\mathrm{mol\,L^{-1}}$). The observed binding constants are in accord with groove binding with DNA as observed in the literature [36]. However, comparing the K_b values of this La(III) complex with those of other known DNA intercalative lanthanide complexes, such as $[LaL_2(NO_3)_3] \cdot 2H_2O$, $(1.97 \pm 0.16) \times 10^5\,\mathrm{mol\,L^{-1}}$; $[SmL(NO_3)_3(C_2H_5OH)] \cdot C_2H_5OH$, $(7.84 \pm 0.32) \times 10^4\,\mathrm{mol\,L^{-1}}$ [37], the La(III) complex of chromone-3-carbaldehyde-(isonicotinoyl) hydrazine, $(4.0 \pm 0.6) \times 10^5\,\mathrm{mol\,L^{-1}}$ [38], the Eu(III) complex of 7-methoxychromone-3-carbaldehyde-(4′-hydroxy) benzoyl hydrazine, $5.11 \times 10^4\,\mathrm{mol\,L^{-1}}$ [39]. It is obvious that the K_b value of the La(III) complex is higher than the above lanthanide DNA intercalators.

In order to further investigate the interaction with CT-DNA, EB(a typical indicator of intercalation) is employed [40]. Figure S3 shows that the maximal absorption of EB at 475 nm (curve A) decreased and shifted to 480 nm (curve B) in the presence of DNA, characteristic of intercalation. Curve C is the absorption of a mixed solution of EB, DNA, and the La(III) complex. The absorption at 488 nm increased as compared with curve B. This could result from two reasons: (1) there may exist a competitive intercalation between the La(III) complex and EB with DNA, so releasing some free EB from the DNA–EB system and (2) EB binds to the La(III) complex strongly, resulting in a decreased amount of EB intercalated into DNA. However, no new absorptions were observed, so the second reason was ruled out.

3.3.2. Fluorescence spectra. Fluorescence titration spectra are effective for characterizing the binding mode of compounds to DNA [41, 42]. The ligand and its La(III) complex emit weak luminescence in Tris-HCl buffer with a maximum wavelength of about 425 nm (figure S4). Compared to the ligand and La(III) complex, the emission

intensity increases with increasing concentrations of DNA, suggesting that the compounds are protected from solvent water by the hydrophobic environment inside the DNA helix and that the La(III) complex can be protected more efficiently than the ligand. Because the hydrophobic environment inside the DNA helix reduces the accessibility of solvent water to the compound and the compound mobility is restricted at certain binding sites, a decrease in the vibrational modes of relaxation results. The fluorescence titration spectra of other intercalators served as references [43]. Consequently, the ligand and its La(III) complex can bind to DNA and the La(III) complex binds more strongly than the free ligand. The higher binding affinity of the La(III) complex is probably attributed to the extension of the π system of the intercalated ligand and coordination of La(III).

The DNA-binding modes were further monitored by a fluorescence EB displacement assay. EB is one of the most sensitive fluorescence probes that can intercalate nonspecifically into DNA and the fluorescence of EB increases after intercalating into DNA base pairs [44]. Competitive binding of other drugs to DNA and EB will result in displacement of bound EB and a decrease in the fluorescence intensity. On the other hand, groove binding of large metal complexes can cause DNA unwinding, EB emission quenching, or binding inhibition with changes in spectroscopy of the metal complex. The emission spectra of EB bound to DNA in the absence and presence of each compound have been recorded for $[EB] = 4 \times 10^{-7}\,mol\,L^{-1}$, $[DNA] = 5 \times 10^{-6}\,mol\,L^{-1}$ with increasing amounts for every compound (figure S5). The addition of the compounds to DNA-bound EB solutions caused obvious reduction in emission intensities and quenching of EB bound to DNA by the ligand and La(III) complex is in good agreement with the linear Stern–Volmer equation. In the plots of F_0/F *versus* $[Q]$, K_q is given by the ratio of the slope to the intercept. The K_q values for the ligand and La(III) complex are $(0.93 \pm 0.03) \times 10^4$ and $(2.36 \pm 0.07) \times 10^4\,mol\,L^{-1}$, respectively. The results show that the interaction of the La(III) complex with DNA is stronger than that of the free ligand, in agreement with the electronic absorption spectral results. The ligand and La(III) complex bind to DNA *via* groove binding and intercalation. Such characteristic change and the K_q value can be observed in some DNA interactions [9, 45].

3.3.3. Viscosity measurements. Intercalation and groove binding can be distinguished by employing hydrodynamic methods, such as viscosity, flow dichroism measurements, and NMR [46]. Hydrodynamic measurements that are sensitive to length change are regarded as the least ambiguous and the most critical tests of binding in solution in the absence of crystallographic structural data [47]. A classical intercalation model demands that the DNA helix lengthens as base pairs are separated to accommodate the binding ligand, leading to an increase in DNA viscosity. In contrast, complexes that bind in the DNA grooves by partial and/or non-classical intercalation typically cause less obvious or no change in DNA solution viscosity [48, 49]. Hence, the viscosity study clarifies the binding of these compounds with DNA. When increasing the amount of the compounds, the relative viscosities of the DNA increase steadily (figure S6). Viscosity measurement shows that the compounds intercalate between adjacent DNA base pairs, causing an extension in the helix and thus increase the viscosity of DNA. There may be some groove binding ability here. The La(III) complex binds more strongly than the

free ligand, leading to greater increase in viscosity of the DNA. The results obtained from the viscosity studies validate those obtained from the spectroscopic studies.

On the basis of all the spectroscopic studies together with the viscosity measurements, the ligand and its La(III) complex are proved to bind to DNA in both groove binding and intercalation mechanism, and the La(III) complex binds to DNA more strongly than the ligand.

3.4. *Hydroxyl radical scavenging activity*

Since the synthesized ligand and its La(III) complex exhibit good DNA binding, we considered it worth investigating other biological activities, such as antioxidant activity. ROS, such as superoxide anion and hydroxyl radical, are usually generated by all aerobic cells during normal oxygen metabolism, and the oxidation induced by ROS is involved in the pathogenesis of various diseases through direct effects on DNA directly and by acting as a tumor promoter [50]. Consequently, in this article, the antioxidant activity of the ligand and its La complexes is studied by comparing their scavenging effects on hydroxyl radical ($HO^{\bullet}$) in KH_2PO_4-Na_2HPO_4 buffer solution.

The inhibitory effect of the compounds is marked and the average suppression ratio for $HO^{\bullet}$ increases with increasing compound concentration (figure S7). The values of IC_{50} of the ligand, the La(III) complex, $La(NO_3)_3$, and mannitol for hydroxyl radical scavenging effects are 22.75, 5.55, 31.62, and 10.19 μmol L^{-1}, respectively (table S4), indicating that formation of metal–ligand coordination complex enhances the scavenger effect and the rare earth metal ions also affect scavenger ability.

4. Conclusion

A ligand, PMFP-isonicotinoyl hydrazone, and its La(III) complex were prepared. The structure of the La(III) complex was determined by X-ray single-crystal diffraction. The DNA-binding properties of the ligand and the complex were investigated by electronic absorption titration, fluorescence spectra, and viscosity measurements. The ligand and La(III) complex bind to DNA *via* groove binding and intercalation. Both ligand and La(III) complex have antioxidation abilities for hydroxyl radicals with the La(III) complex showing stronger scavenging effects than ligand. Information obtained from this work may be helpful to the development of biological, pharmaceutical, and physiological applications.

Supplementary material

Supplementary data associated with this article can be found in the online version. CCDC 795294 contains the supplementary crystallographic data for this article. These data can be obtained free of charge from The Cambridge Crystallographic Data Centre *via* www.ccdc.cam.ac.uk/data_request/cif.

Acknowledgment

This work is supported by the National Natural Science Foundation of China (20975046).

References

[1] G. Facchini, E. Kremer. *Polyhedron*, **28**, 2329 (2009).
[2] A.E. Friedman, C.V. Kumar. *Nucleic Acids Res.*, **19**, 2595 (1991).
[3] C. Zimmer, U. Wahnert. *Prog. Biophys. Mol. Biol.*, **47**, 31 (1986).
[4] N.T. Thuong, C. Hélène. *Angew. Chem. Int. Ed. Engl.*, **32**, 666 (1993).
[5] P.B. Dervan, B.S. Edelson. *Curr. Opin. Struct. Biol.*, **13**, 284 (2003).
[6] L.P.G. Wakelin. *Med. Res. Rev.*, **6**, 275 (1986).
[7] B.H. Geierstanger, D.E. Wemmer. *Annu. Rev. Biophys. Biomol. Struct.*, **24**, 463 (1995).
[8] H. Zhang, C.S. Liu, X.H. Bu, M. Yang. *J. Inorg. Biochem.*, **99**, 1119 (2005).
[9] B.D. Wang, Z.Y. Yang, Q. Wang, T.K. Cai, P. Crewdson. *Bioorg. Med. Chem.*, **14**, 1880 (2006).
[10] B.D. Wang, Z.Y. Yang, D.D. Qin, Z.N. Chen. *J. Photochem. Photobiol. A: Chem.*, **194**, 49 (2008).
[11] B.D. Wang, Z.Y. Yang, T.R. Li. *Bioorg. Med. Chem.*, **14**, 6012 (2006).
[12] M.F. Iskander, L. Sayed, A.F.M. Hefny, S.E. Zayan. *J. Inorg. Nucl. Chem.*, **38**, 2209 (1976).
[13] H. Adams, D.E. Fenton, G. Minardi, E. Mura, M. Angelo. *Inorg. Chem. Commun.*, **3**, 24 (2000).
[14] Z.Y. Yang, R.D. Yang, F.S. Li, K.B. Yu. *Polyhedron*, **19**, 2599 (2000).
[15] Z.Y. Yang, B.D. Wang, Y.H. Li. *J. Organomet. Chem.*, **691**, 4159 (2006).
[16] H.G. Li, Z.Y. Yang, B.D. Wang, J.C. Wu. *J. Organomet. Chem.*, **695**, 415 (2010).
[17] İlhami Gülcin. *Life Sci.*, **78**, 803 (2006).
[18] S.S. Leonard, D. Keil, T. Mehlmanb, S. Proper, X. Shi, G.K. Harris. *J. Ethnopharmacol.*, **103**, 288 (2006).
[19] Y.Z. Cai, Q. Luo, M. Sun, H. Corke. *Life Sci.*, **74**, 2157 (2004).
[20] K.E. Heim, A.R. Tagliaferro, D.J. Bobilya. *J. Nutr. Biochem.*, **13**, 572 (2002).
[21] D.J. Wallace, J.M. Straley. *Org. Chem.*, **26**, 3825 (1961).
[22] H.G. Li, Z.Y. Yang, D.D. Qin. *Inorg. Chem. Commun.*, **12**, 494 (2009).
[23] M.R. Eftink, C.A. Ghiron. *Anal. Biochem.*, **114**, 199 (1981).
[24] M. Eriksson, M. Leijon, C. Hiort, B. Norden, A. Graeslund. *Biochemistry*, **33**, 5031 (1994).
[25] Y. Xiong, X.F. He, X.H. Zou, J.Z. Wu, X.M. Chen, L.N. Ji, R.H. Li, J.Y. Zhou, K.B. Yu. *J. Chem. Soc., Dalton. Trans.*, **1**, 19 (1999).
[26] C.C. Winterbourn. *Biochem. J.*, **198**, 125 (1981).
[27] X.M. Chen, J.W. Cai (Eds.), *Single-Crystal Structural Analysis*, *Principles and Practices*, Science Press, Beijing (2003).
[28] W.J. Geary. *Coord. Chem. Rev.*, **7**, 81 (1971).
[29] M.F. Iskander, L. El-sayed, N.M.H. Salem, W. Haase, H.J. Linder, S. Foro. *Polyhedron*, **23**, 23 (2004).
[30] G.C. Xu, L. Zhang, L. Liu, G.F. Liu, D.Z. Jia. *Polyhedron*, **27**, 12 (2008).
[31] K.K. Narang, V.P. Singh. *Transition Met. Chem.*, **18**, 287 (1993).
[32] F. Maarchetti, C. Pettinari, R. Pettinari, D. Leonesi, A. Lorenzotti. *Polyhedron*, **18**, 3041 (1999).
[33] B.D. Wang, Z.Y. Yang, D.W. Zhang, Y. Wang. *Spectrochim. Acta, Part A*, **63**, 213 (2006).
[34] J.K. Barton, A. Danishefsky, J. Goldberg. *J. Am. Chem. Soc.*, **106**, 2172 (1984).
[35] H. Xu, K.C. Zheng, L.J. Lin, H. Li, Y. Gao, L.N. Ji. *J. Inorg. Biochem.*, **98**, 87 (2004).
[36] Z.H. Xu, P.X. Xi, F.J. Chen, Z.Z. Zeng. *J. Coord. Chem.*, **62**, 2193 (2009).
[37] Q. Wang, Z.Y. Yang, G.F. Qi, D.D. Qin. *Biometals*, **22**, 927 (2009).
[38] Y. Li, Z.Y. Yang. *J. Coord. Chem.*, **63**, 1960 (2010).
[39] Q. Wang, Z.Y. Yang, G.F. Qi, D.D. Qin. *Eur. J. Med. Chem.*, **44**, 2425 (2009).
[40] W.D. Wilson, L. Ratmeyer, M. Zhao, L. Stekowshi, D. Boykin. *Biochemistry*, **32**, 4098 (1993).
[41] G. Zhao, H. Lin, S. Zhu, H. Sun, Y. Chen. *J. Inorg. Biochem.*, **70**, 219 (1998).
[42] M. Howe-Grant, K.C. Wu, W.R. Bauer, S.J. Lippard. *Biochemistry*, **15**, 4339 (1976).
[43] T.R. Li, Z.Y. Yang, B.D. Wang, D.D. Qin. *Eur. J. Med. Chem.*, **43**, 1688 (2008).
[44] J.B. Le-Pecq, C. Paoletti. *J. Mol. Biol.*, **27**, 87 (1967).
[45] C.V. Kumar, J.K. Barton, N.J. Turro. *J. Am. Chem. Soc.*, **107**, 5518 (1985).
[46] L. Strekowski, B. Wilson. *Mutation Res.*, **623**, 3 (2007).
[47] S. Satyanarayana, J.C. Dabrowiak, J.B. Chaires. *Biochemistry*, **32**, 2573 (1993).
[48] J.J. Marmur. *J. Mol. Biol.*, **3**, 208 (1961).
[49] C.V. Kumar, E.H. Asuncion. *J. Am. Chem. Soc.*, **115**, 8547 (1993).
[50] R.M. Towyz. *Hypertension*, **44**, 248 (2004).